Climatology and spectral characteristics of 10-day rainfall variability in Manokwari, West Papua (1991–2022)

Aries Subgan[1]*, *Adi* Mulsandi[2], and *Munawar*[3]

[1] Physics Department, Faculty of Mathematics and Natural Sciences, University of Papua, 98314, Manokwari, Indonesia
[2] Meteorology Study Program, Sekolah Tinggi Meteorologi Klimatologi dan Geofisika (STMKG), 15119, Tangerang City, Indonesia
[3] Climatology Study Program, Sekolah Tinggi Meteorologi Klimatologi dan Geofisika (STMKG), 15119, Tangerang City, Indonesia

Abstract. Rainfall variability in the Indo-Pacific warm pool arises from coupled interactions between the Intertropical Convergence Zone (ITCZ), the Asian–Australian monsoon, and large-scale ocean–atmosphere teleconnections. However, eastern Indonesia, particularly West Papua, remains underrepresented in climatological research. This study examined rainfall dynamics in Manokwari, West Papua, using 32 years (1991–2022) of BMKG station observations. Daily rainfall was aggregated into dekadal (10-day) totals to capture variability from intraseasonal to interannual timescales. We first characterized the annual and seasonal rainfall cycles using descriptive statistics and then diagnosed the dominant periodicities through Fast Fourier Transform (FFT) spectral analysis. To assess large-scale climate control, we quantified relationships between dekadal rainfall and key climate drivers, El Niño–Southern Oscillation (ENSO), the Indian Ocean Dipole (IOD), and the Australian monsoon, using correlation and partial correlation analyses to isolate each driver's independent association amid overlapping signals. Together, these diagnostics establish a robust dekadal climatology for an equatorial maritime region with limited prior analysis, supporting seasonal monitoring and climate-sensitive decision making. Beyond site-specific findings, this study introduces a replicable central–local co-production approach: standardized diagnostics developed centrally are paired with locally owned station data and locally contextualized interpretation by forecasters in the field. Applied across stations, this framework can strengthen the local analytical capacity in remote regions while improving the consistency and depth of Indonesia's climate information services for adaptation and operational forecasting, with ENSO emerging as the most robust large-scale modulator in both partial-correlation and phase-composite evidence.

1 Introduction

Rainfall variability in the tropics is a central issue in climate science because it governs hydrological cycles [1], agricultural productivity [2], and disaster risk in some of the most densely populated and climate-sensitive regions of the world [3]. Unlike temperate zones, where rainfall is largely modulated by mid-latitude dynamics, equatorial rainfall is shaped by a superposition of processes that operate across multiple timescales, ranging from intraseasonal oscillations to interannual anomalies [4], [5]. In particular the Indo-Pacific warm pool is one of the most dynamic regions on Earth, where the Intertropical Convergence Zone (ITCZ), the Asian–Australian monsoon system, and ocean–atmosphere teleconnections converge to generate complex rainfall regimes.

Eastern Indonesia is at the heart of this hydroclimatic nexus. Its geographical position between the Pacific and Indian Oceans exposes the region to a variety of climatic drivers that act simultaneously or sequentially, often producing nonlinear and region-specific rainfall responses [6], [7]. While substantial attention has been devoted to rainfall variability in western Indonesia, such as Java, Sumatra, and Sulawesi, eastern provinces such as West Papua, remain comparatively underexamined. This imbalance in spatial coverage has limited a full understanding of the Indonesian rainfall system, particularly in maritime equatorial settings, where rainfall seasonality deviates from the classic monsoon-dominated pattern.

One of the key challenges in characterizing tropical rainfall is identifying variability at intermediate timescales [8]. Daily data often emphasize weather-scale noise, whereas monthly averages can obscure intraseasonal and seasonal transitions. The dekadal (10-day) scale, recommended in tropical climatology, provides an effective compromise by retaining the signals of the ITCZ passage, monsoon fluctuations, and teleconnection influences without being overwhelmed by synoptic-scale disturbances. However, despite its relevance for both scientific analysis and practical applications, such as agricultural planning, dekadal climatology remains underutilized in rainfall studies in eastern Indonesia.

Another critical dimension in advancing rainfall studies is the explicit examination of periodicity and its

* Corresponding: a.subgan@unipa.ac.id

linkage to large-scale climatic modes. Spectral analysis provides a diagnostic lens to reveal recurring cycles beyond the conventional seasonal framework, highlighting the influence of harmonics and low-frequency modulations [9], [10]. Combined with correlation approaches that disentangle overlapping drivers, such as ENSO, the Indian Ocean Dipole (IOD), and the Australian monsoon, such methods can shed light on the relative contributions of each climate mode to rainfall variability.

Given the dual importance of Manokwari as a representative equatorial maritime climate zone and as a region highly dependent on reliable rainfall for livelihoods, there is a compelling need to establish a robust climatological baseline of rainfall variability at multiple timescales. Beyond filling the geographical gap in the literature, such work is crucial for improving seasonal outlooks, guiding water resource management, and informing climate adaptation in eastern Indonesia.

Accordingly, this study pursues three objectives: (i) to document the long-term rainfall climatology in Manokwari using dekadal aggregation, (ii) to analyze periodic components of rainfall variability through spectral diagnostics, and (iii) to assess the influence of major climate modes, particularly ENSO, IOD, and Australian monsoon, using correlation-based approaches. By addressing these objectives, this study sought to provide new insights into the hydroclimatic dynamics of eastern Indonesia and contribute to the broader discourse on tropical rainfall variability.

2 Materials and Method

2.1 Data source and dekadal aggregation (10-day scale)

This study used 32 years of daily rainfall records (1991–2022) from the BMKG station in Manokwari, West Papua. Daily rainfall was aggregated into dekadal (10-day) totals following the WMO Convention (36 dekads per year). A 10-day scale was selected for three reasons. First, it provides an intermediate temporal resolution that reduces synoptic "weather noise" present in daily series while retaining intraseasonal and seasonal transition signals that are often smoothed out by monthly means. Second, dekadal aggregation offers a practical compromise for equatorial maritime regimes, where rainfall seasonality is subtle and transition periods can occur within weeks. Third, the dekadal format aligns with operational climate monitoring and services in which 10-day summaries are widely used as interpretable unit for situational awareness and planning in regions with limited dense observations.

In addition to rainfall, three large-scale climate indices were analyzed as potential modulators of variability: the Niño 3.4 index representing the ENSO; the Australian Monsoon Index (AUSMI) capturing monsoonal circulation strength; and the Dipole Mode Index (DMI) as a measure of the Indian Ocean Dipole (IOD). The monthly values of these indices were obtained from international climate data repositories and synchronized with the rainfall time series.

Analytical procedures were designed to capture multiple scales of variability. Long-term statistics, including means, standard deviations, and anomalies, were computed to characterize the annual and interannual fluctuations. Dekadal climatology was constructed from multi-year averages to identify the timing of rainfall peaks and occurrence of a dry season. The onset, retreat, and wet-season lengths were determined using rainfall thresholds commonly applied in Indonesian climatological studies.

2.2 Quality control (QC) and completeness criteria

Prior to aggregation and analysis, the daily rainfall data were subjected to basic QC procedures to reduce non-climatic artifacts. QC included (i) format and consistency checks (date continuity and duplicate records), (ii) range checks (flagging physically implausible negative values and extreme outliers for re-verification), and (iii) missing-data screening at daily and dekadal levels. Dekadal totals were computed only for dekads with sufficient daily coverage. Dekads failing the completeness criterion were treated as missing and excluded from climatological averaging to avoid bias. These steps ensure that the derived climatology, extremes, and teleconnection statistics are not driven by data gaps or isolated recording artifacts.

2.3 Spectral analysis and its limitations; comparison with alternative methods

Dominant periodicities in the dekadal rainfall series were diagnosed using the Fast Fourier Transform (FFT) to summarize the variance across frequency bands (seasonal harmonics, intraseasonal variability, and low-frequency modulation). The FFT was chosen because the dekadal series is regularly spaced and sufficiently long (32 years) to resolve the key timescales of interest, providing an interpretable first-order spectrum. Nevertheless, FFT has important limitations: it assumes (quasi-)stationarity of the underlying process over the full record, can be affected by spectral leakage and edge effects in finite samples, and provides limited time localization (i.e., it does not indicate when a given frequency band is most active). For this reason, FFT results are interpreted as time-mean spectral characteristics rather than evidence of temporally invariant oscillations [11], [12].

Other approaches could complement FFT in future work, such as wavelet transforms (time–frequency localization for nonstationary intraseasonal variability), multi-taper spectral methods (reduced leakage and more robust peak estimation), and Lomb–Scargle periodograms when irregular sampling or substantial missingness prevents standard FFT application. In the present study, FFT served as a transparent baseline diagnostic, while teleconnection attribution was strengthened through correlation and partial correlation analyses that isolated independent associations among ENSO, IOD, and monsoon indices.

Extreme rainfall was examined by isolating dekads that exceed the 95th percentile of the distribution. The temporal distribution of these events was assessed in both the dekadal and monthly dimensions, and their intensity was summarized using distributional statistics [13]–[15]. The single wettest dekad for each year was further extracted to capture the interannual fluctuations in extreme intensity.

The influence of large-scale climate drivers was evaluated using correlation techniques. Pairwise Pearson correlations were applied to assess the direct associations between rainfall and each climate index. A partial correlation analysis was then conducted to isolate the independent contribution of ENSO, AUSMI, and IOD by controlling for shared variability. Statistical significance was evaluated at the 95% confidence level to ensure the robustness of the findings.

3 Results and Discussion

3.1 Annual Rainfall Statistics

The total annual rainfall in Manokwari during 1991–2022 exhibited substantial variability from year to year. The mean annual rainfall is 2185.98 mm, with a standard deviation of 458.76 mm, indicating relatively high interannual fluctuation in rainfall amounts. The driest year within the record occurred in 2004, with 1408.69 mm, while the wettest year was 2017, when annual rainfall reached 3288.28 mm. These values suggest that the annual totals can deviate by more than ±30% from the long-term mean.

The interannual variability is illustrated in Fig. 1, where no persistent long-term upward or downward trends are visually evident. Instead, rainfall fluctuated markedly between relatively wet and dry years.

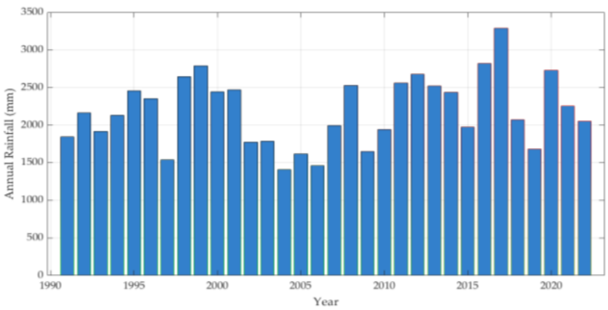

Fig. 1. Annual rainfall totals in Manokwari, West Papua, during 1991–2022.

3.2 Spectral Diagnostics of 10-day Rainfall

The power spectrum of the 10-day (dekadal) rainfall series highlights dominant variability bands in Manokwari (Fig. 2), including a strong annual peak (~365 d), a clear semi-annual harmonic (~180 d), and pronounced intraseasonal energy centered near ~90 d with broader power across ~30–90 d. A lower-frequency shoulder is also present around the 2–3-year band.

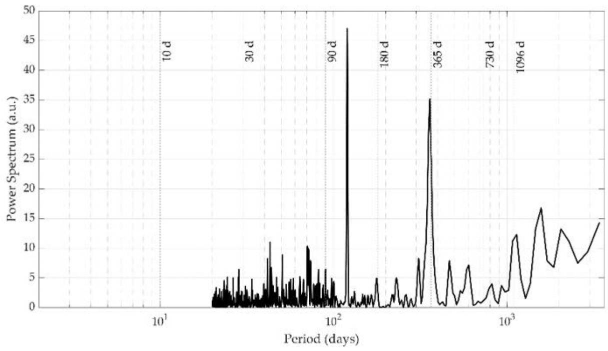

Fig. 2. Power spectrum of dekadal rainfall in Manokwari (log-period axis). Vertical guides mark 10, 30, 90, 180, 365, 730, and 1096 days. The spectrum shows dominant peaks near ~365 d (annual) and ~180 d (semi-annual), substantial power across ~30–90 d intraseasonal periods, and a lower-frequency shoulder in the ~2–3-year band.

3.3 Annual Cycle of Rainfall (10-day Climatology)

The 10-day rainfall climatology for Manokwari (1991–2022) exhibited a semiannual structure with two prominent rainfall peaks (Fig. 3). The first maximum occured during April, the second dekad (Apr-2), with a mean rainfall of approximately 85 mm per dekad, while the second peak appeared in August, the second dekad (Aug-2), with a mean rainfall of approximately 75 mm per dekad. Between these peaks, rainfall decreased temporarily, forming relative minima within the annual cycle. The shaded envelope in Fig. 3 (±1 standard deviation) indicates substantial interannual variability, with the largest spread occurring during the peak periods.

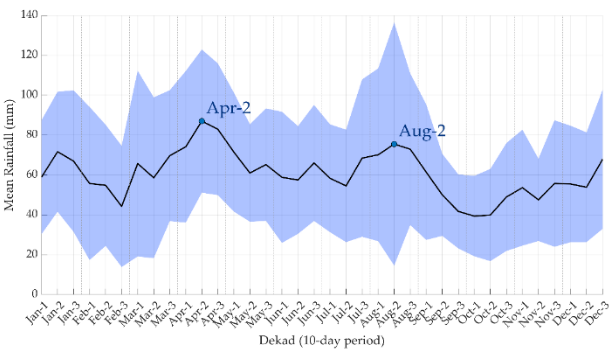

Fig. 3. Ten-day rainfall climatology in Manokwari, West Papua (1991–2022). The solid line represents the long-term mean, and the shaded area indicates ±1 standard deviation. Two rainfall maxima occur around April (second dekad) and August (second dekad), with a temporary decrease between peaks.

3.4 Dekadal Rainfall Climatology

The 32-year dekadal climatology indicates an equatorial rainfall regime, with precipitation sustained through most of the year. Only one short dry window was evident, centered in October (dekads 28–30), which consistently exhibited the lowest mean rainfall (Fig. 4). In other months, the dekadal mean rainfall remained substantially higher, indicating that the region experienced a single, brief dry season embedded within a predominantly wet annual cycle.

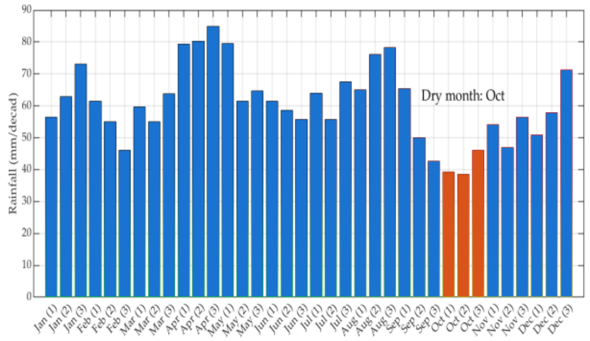

Fig. 4. Multi-year (32-year) mean dekadal rainfall climatology in Manokwari from January (dekad 1) to December (dekad 36). Bars indicate mean rainfall (mm per dekad); highlighted bars mark October (dekads 28–30), which shows the lowest mean rainfall relative to other dekads.

3.5 Interannual Variability and Long-Term Trend

Fig. 5 summarizes the year-to-year departures from the 32-year mean for the key hydroclimate metrics. Annual rainfall and wet-season total anomalies co-vary closely (panels a–b, Fig. 5), and their 3-year running means trace similar multi-year swings. Peaks and troughs in wet-season totals (panel b) were not accompanied by proportional shifts in the onset or retreat timing.

Anomalies of onset and retreat (panels c–d, Fig. 5) were generally centered near zero and remain within only a few dekads of the mean, with episodic early/late seasons rather than a persistent drift. Years with later onset often exhibit a later retreat, indicating partial compensation between the two ends of the season.

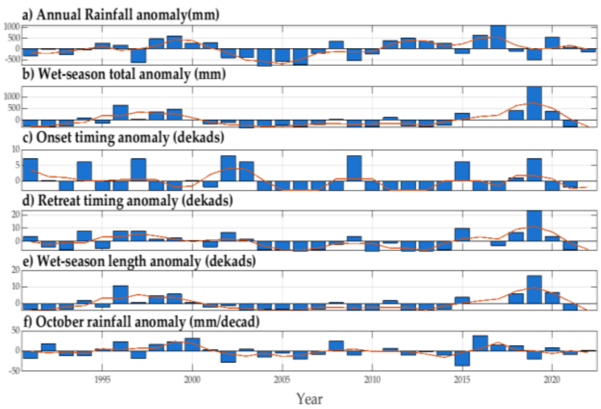

Fig. 5. Interannual anomalies (bars) with 3-year running mean (thin orange line) for: (a) annual rainfall (mm), (b) wet-season total (mm), (c) onset timing (dekads), (d) retreat timing (dekads), (e) wet-season length (dekads), and (f) October rainfall (mm per dekad). Anomalies are computed relative to the 32-year mean. Onset and retreat are measured in dekads of the hydrologic year (September–August).

Consistent with this behavior, variability in wet-season length was comparatively modest (panel e, Fig. 5), as changes in onset and retreat largely offset one another. October rainfall anomalies (panel f, Fig. 5) show a broad alignment with timing metrics: negative October anomalies tend to coincide with later onsets or shorter seasons, whereas positive October anomalies accompany earlier onsets or longer seasons.

3.6 Extreme Rainfall Characteristics

Fig. 6 shows the interannual variability in both the magnitude of the wettest dekad each year (panel a) and the timing the peak occurence (panel b). Wettest-dekad totals vary by more than a factor of two across years. The timing clusters primarily in late boreal summer to early boreal autumn (dekads ~20–24), with a secondary occurrence in late boreal spring (dekads ~9–12), whereas very early or very late occurrences are rare.

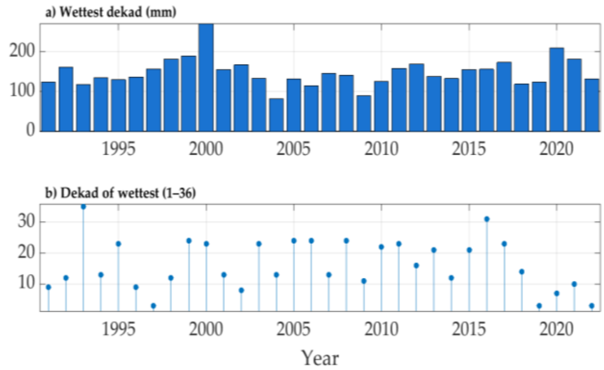

Fig. 6. (a) Wettest-dekad rainfall (mm) for each year; (b) dekad index (1–36) of the wettest dekad. Dekad 1–36 corresponds to Jan(1)…Dec(3).

Fig. 7 summarizes the seasonal timing of extreme dekadal events (≥95th percentile of the full dekadal series). In the dekad space (top panel), extremes concentrate around dekads 20–24, and in the month space (bottom panel) they peak in April and August, with relatively few events in October.

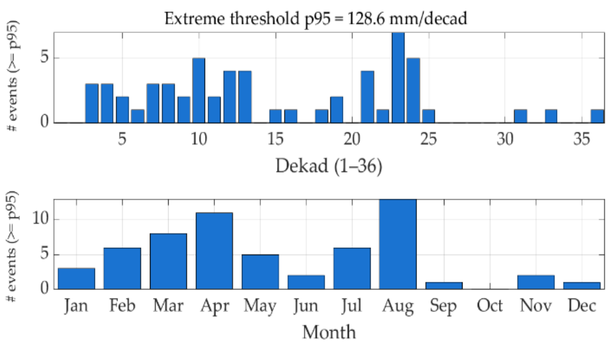

Fig. 7. Timing distribution of extreme dekadal rainfall events defined by the 95th percentile of the full dekadal dataset: (top) counts by dekad (1–36); (bottom) counts by calendar month.

Fig. 8 presents the monthly intensity distribution of extreme dekadal rainfall. The median and interquartile ranges were largest in June–August, while September–November exhibited fewer events and generally lower extreme intensities. The dashed line denotes the 95th-percentile threshold used to define extremes.

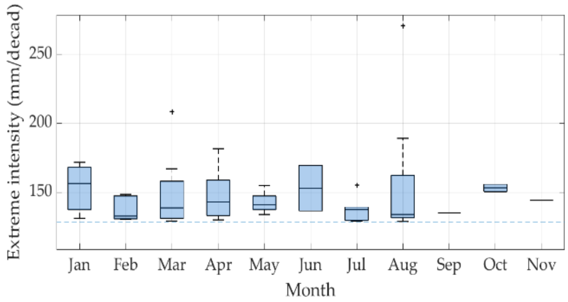

Fig. 8. Boxplots of extreme dekadal rainfall (≥95th percentile) by calendar month. Boxes show median and interquartile range, whiskers the 1.5×IQR, and symbols the outliers. The dashed horizontal line indicates the 95th-percentile threshold used to define extremes.

3.7 Monsoon and Oceanic Controls: Pairwise vs. Partial Correlations

Using monthly data (N = 384), we examined the associations between rainfall and three climate indices: the Australian Monsoon Index (AUSMI), Niño-3.4 (ENSO), and the Indian Ocean Dipole (IOD). Pairwise correlations quantified raw associations, whereas partial correlations estimated the association of each index with rainfall while controlling for the other two (Table 1).

Pairwise correlations show a negative relationship between rainfall and Niño-3.4 ($r = -0.238$, $p = 2.3\times10^{-6}$). AUSMI exhibited a small positive correlation that was not statistically significant ($r = 0.076$, $p = 0.138$), wereas IOD showed a weak negative correlation ($r = -0.110$, $p = 0.031$).

Partial correlations indicate that Niño-3.4 remains significantly associated with rainfall after controlling for AUSMI and IOD (r_partial = −0.209, $p = 3.8\times10^{-5}$). In contrast, AUSMI approached zero and was non-significant (r_partial = 0.003, p = 0.952), and IOD became non-significant (r_partial = −0.027, p = 0.596) (Table 1).

Table 1. Pairwise (r_pair) and partial (r_partial) correlations between monthly rainfall and AUSMI, Niño-3.4, and IOD (*N*=384 months).

Variable	r pair	p pair	r partial	p partial	N
AUSMI	0.08	0.14	0.003	0.95	384
NINO34	-0.24	2.31E-06	-0.209	3.81E -05	384
IOD	-0.11	0.03	-0.027	0.59	384

3.8 ENSO-Phase Composite in JJA and Group Differences

To provide an explicit phase-based comparison, we computed ENSO composites for the boreal summer (JJA) and tested whether rainfall differs among El Niño, Neutral, and La Niña conditions (Fig. 9). The JJA composite indicates higher mean rainfall during La Niña (n = 15; mean = 231.90 mm; SD = 94.20) than during Neutral conditions (n = 62; mean = 197.07 mm; SD = 75.64), while El Niño shows the lowest mean rainfall (n = 19; mean = 155.42 mm; SD = 77.60). Assumption checks supported the use of parametric testing: Shapiro–Wilk tests did not reject normality for any group (all $p > 0.05$) and Levene's test indicated homogeneity of variance ($p = 0.580$). A one-way ANOVA confirmed a statistically significant difference among the ENSO phases ($F = 4.03$, $p = 0.021$), with a small-to-moderate effect size ($\eta^2 = 0.080$). Robust Welch ANOVA yielded a consistent result ($p = 0.043$), supporting the phase-dependent contrast observed in the composites.

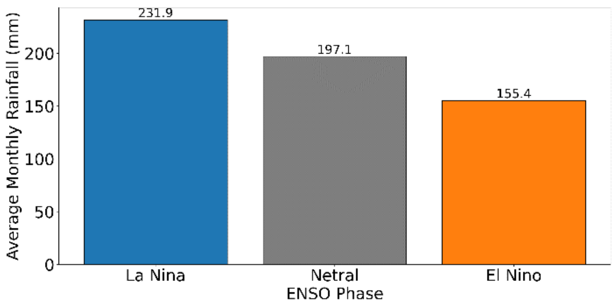

Fig. 9. Mean JJA rainfall composites (mm) in Manokwari by ENSO phase (La Niña, Neutral, El Niño) for 1991–2022. The phase contrast is evaluated using one-way ANOVA as reported in Section 3.8.

3.9 Discussion

3.9.1 Seasonal structure and ITCZ-linked transitions in an equatorial maritime regime

Manokwari exhibits a predominantly wet equatorial rainfall regime, yet a recurrent short dry window in October emerges consistently in dekadal climatology. This feature is operationally important because short but repeatable dry periods can be obscured when rainfall is summarized only at monthly resolution. The dekadal annual cycle also shows two rainfall maxima (around April and August), indicating that the rainfall peaks are concentrated during the seasonal transition phases.

A plausible physical interpretation is the twice-yearly migration of the ITCZ across the region, which can enhance convection and low-level convergence during the boreal spring and late boreal summer. The unequal amplitudes of the two peaks may reflect asymmetries in background circulation and moisture availability across the annual cycle, whereas the persistence of a single brief dry window in October highlights the nonlinearity of the equatorial hydroclimate.

Interannual anomalies further indicate that year-to-year differences in rainfall totals are driven primarily by changes in wet-season intensity rather than by systematic shifts in onset and retreat timing. Consistent with this, the timing of the wettest dekad clusters mainly in dekads ~20–24 with a secondary occurrence in dekads ~9–12, reinforcing that extremes tend to occur within or near the climatological peak phases rather than during the October dry window. These seasonal-structure insights provide a context for interpreting the dominant role of large-scale climate variability as discussed in the following section.

3.9.2 Interpreting the spectrum: harmonics, intraseasonal variability, and low-frequency modulation

The spectrum provides a multiscale context for interpreting rainfall variability in Manokwari. In equatorial maritime settings, harmonic energy can arise even when the mean annual cycle does not exhibit two distinct dry seasons; therefore, the semi-annual peak is best interpreted as a manifestation of the transition structure and a non-sinusoidal annual cycle rather than as evidence of two separate dry regimes. In this setting, the semi-annual signal may be reinforced by sharp wet–dry transitions and intraseasonal modulation (e.g., BSISO/MJO), which can add harmonic power without producing bimodal dry-season climatology. The enhanced variance at intraseasonal periods (~30–90 days) is consistent with the week-to-month modulation of convection, while the presence of a 2–3-year band provides a timescale-consistent backdrop for ENSO-related modulation as discussed in the teleconnection results. Overall, the spectrum links the seasonal structure (Sections 3.3–3.4) to the characteristic timescales at which regional-to-large-scale variability can influence local rainfall.

3.9.3 Why ENSO emerges as the dominant large-scale controller

Multiple lines of evidence indicate that ENSO is the dominant large-scale modulator of rainfall variability in Manokwari. Pairwise correlations show a negative rainfall–Niño3.4, and the partial-correlation results are especially informative because ENSO retains a robust association with rainfall even after controlling for the Australian monsoon index (AUSMI) and Indian Ocean Dipole (IOD). This supports an independent ENSO contribution rather than a relationship driven primarily by the shared covariance among the climate modes. The distinction matters because pairwise correlations alone can overstate the role of covarying drivers under seasonal and interannual coupling; in the present results, the explanatory role of AUSMI and IOD is markedly reduced once ENSO is accounted for, suggesting that their statistical signals largely reflect co-variability with ENSO, even if they may still influence rainfall indirectly through broader Indo-Pacific circulation.

The interannual anomaly structure provides a consistent interpretation: variability is largest during peak periods, indicating that year-to-year changes primarily modulate wet-season intensity and accumulation rather than systematically restructuring the timing of the climatological cycle. In combination, these results indicate that ENSO is the most robust independent large-scale influence at the site on the analyzed timescales.

3.9.4 ENSO phase composites in JJA: intuitive evidence consistent with statistical attribution

The ENSO-phase composite analysis for JJA strengthens this attribution by translating the correlation structure into an intuitive phase-based comparison. Mean JJA rainfall is highest during La Niña conditions ($n = 15$; mean = 231.90 mm; SD = 94.20), intermediate during neutral years ($n = 62$; mean = 197.07 mm; SD = 75.64), and lowest during El Niño ($n = 19$; mean = 155.42 mm; SD = 77.60). Assumption checks supported parametric comparison (Shapiro–Wilk $p > 0.05$, for all groups; Levene $p = 0.580$), and one-way ANOVA indicated statistically significant differences among phases ($F = 4.03$, $p = 0.021$) with a small-to-moderate effect size ($\eta^2 = 0.080$). A Welch ANOVA yielded consistent significance ($p = 0.043$), suggesting that phase contrast is robust to variance assumptions. Together, these results provide converging evidence with the partial-correlation analysis that ENSO is a primary large-scale modulator of the JJA rainfall intensity in Manokwari.

3.9.5 Implications for forecasting practice and climate services: from local insight to national consistency

Beyond site-specific climatology, the value of this study lies in how the results can be operationalized and transferred. The combination of dekadal aggregation, multiscale diagnostics (seasonal statistics and spectral characterization), and driver-focused attribution provides a replicable workflow that can be used by forecasters in remote stations to sharpen local understanding while maintaining analytical consistency with centrally validated approaches. The demonstrated ENSO dependence further suggests that routinely issued ENSO outlooks can be translated into locally grounded narratives in dekadal-to-seasonal horizons. Applied across stations, such workflows can strengthen the local analytical capacity and, by accumulation, improve the consistency and depth of Indonesia's climate information services.

Operationally, these results highlight several decision-relevant timing cues. First, monitoring should emphasize within-season rainfall accumulation and intensity because interannual differences in seasonal totals are not necessarily accompanied by large shifts in onset/retreat timing. Second, extreme dekadal rainfall is most likely to occur around seasonal transition months (notably April and August), whereas October shows comparatively few extremes; this seasonality provides practical "risk windows" for heightened monitoring and preparedness. Finally, the broader spread of extreme intensities in mid-year (June–August) indicates that extremes are not only more frequent but also more variable in magnitude, which can complicate short-horizon planning and warrants careful attention.

3.9.6 Limitations and future directions

This study had several limitations. First, ENSO composites and phase-based statistics depend on the sample sizes within each category, and the magnitude of phase contrasts may be sensitive to the ENSO classification metric and the seasonal window adopted. Second, FFT summarizes time-mean spectral characteristics and does not localize variability in time; potential nonstationarity and event-driven changes should be better examined using time–frequency approaches (e.g., wavelet analysis) or other robust spectral estimators in future work. Third, the present study is primarily statistical; incorporating circulation diagnostics (e.g., low-level winds, moisture flux convergence, and convective indices) would strengthen mechanistic attribution and early warning relevance, including a clearer dynamical fingerprint of monsoon influence that may not be fully captured by a single monthly AUSMI index. Extending the analysis to these dynamical fields and evaluating consistency against reanalysis or model outputs would help translate the identified dekadal risk windows into more process-informed forecast guidance.

4 Conclusions

This study provides a comprehensive characterization of the rainfall climatology and variability in Manokwari, West Papua, based on a 32-year Dekadal dataset (1991–2022). Manokwari exhibits a predominantly wet equatorial regime with a single, recurrent dry window in October, while annual totals vary markedly (approximately 1400–3200 mm), driven mainly by changes in wet-season intensity, rather than by systematic shifts in onset or retreat timing.

Spectral diagnostics showed dominant annual and semi-annual harmonics, substantial intraseasonal variability (30–90 days), and low-frequency modulation in the 2–3-year band, consistent with ENSO-scale variability. The semi-annual component is consistent with ITCZ-linked seasonal transitions; however, operationally, the climatology features only one brief dry month. Extreme rainfall characteristics indicated that the wettest dekads clustered around April and August, whereas October remained consistently dry.

Teleconnection diagnostics identify ENSO as the most robust large-scale modulator of rainfall in Manokwari: Niño-3.4 remains significantly associated with rainfall after controlling for AUSMI and IOD, and the ENSO phase composites for JJA show systematically wetter conditions during La Niña and drier conditions during El Niño. The apparent monsoon and IOD relationships are reduced once ENSO is accounted for, indicating substantial shared co-variability rather than distinct independent controls a monthly resolution.

Novelty and Practical Values. Beyond site-specific findings, this study advances a replicable analytical framework for dekadal rainfall in data-sparse eastern Indonesia by combining standardized multiscale diagnostics (seasonal-cycle statistics, FFT-based spectral characterization, and correlation/partial-correlation attribution) with locally owned station observations. The framework supports a central–local co-production workflow in which centrally validated analytical procedures are strengthened through locally contextualized interpretation by forecasters in the field. The resulting dekadal rainfall calendar and risk windows provide decision-relevant guidance for seasonal monitoring, climate-sensitive planning, and preparedness, and, when applied across stations, can cumulatively strengthen the consistency and depth of Indonesia's climate information services.

Future work integrating circulation diagnostics (e.g., low-level winds, moisture flux convergence, and convective indices) and targeted model-based evaluation will further refine the process attribution and improve early warning readiness under ongoing climate variability and change.

References

1. Q. Liu, X. Zhao, H. Wang, and Y. Sun, "Establishment and Analysis of Spatiotemporal Variation Hydrological Model of Distributed Rainfall and Evaporation in Biliu River Basin," *Complexity*. 2021, doi:10.1155/2021/6639691.
2. S. Y. Khedikar, S. N. Panchabhai, and T. K. Mandal, "Study on Effect of Rainfall Variability on Crop Productivity of Tur (Arhar) and Cotton Crops for Various Districts of Maharashtra, India," *International Journal of Environment and Climate Change*. 2023, doi: 10.9734/ijecc/2023/v13i92468.
3. S. Hayashi, M. Kunitomo, K. Mikami, and K. Suzuki, "Recent and Historical Background and Current Challenges for Sediment Disaster Measures Against Climate Change in Japan," *Water*. 2022, doi: 10.3390/w14152285.
4. A. Mulsandi, Y. Koesmaryono, R. Hidayat, A. Faqih, and A. Sopaheluwakan, "Detecting Indonesian Monsoon Signals and Related Features Using Space–Time Singular Value Decomposition (SVD)," *Atmosphere*, vol. 15, no. 2. 2024, doi: 10.3390/atmos15020187.
5. S. Ferrett, G. Yang, S. J. Woolnough, K. Hodges, and C. E. Holloway, "Linking extreme precipitation in Southeast Asia to equatorial waves," no. June 2019, pp. 665–684, 2020, doi: 10.1002/qj.3699.
6. A. A. Subgan, "Analisis Karakteristik Curah Hujan Wilayah Papua Bagian Utara Dan Selatan," *Jurnal Natural*. 2012, doi: 10.30862/jn.v9i2.326.
7. A. Mulsandi, Y. Koesmaryono, R. Hidayat, A. Faqih, and A. Sopaheluwakan, "On The Interannual Variability of Indonesian Monsoon Rainfall (IMR): A Literature Review of The Role of its External Forcing," *J. Meteorol. dan Geofis.*, vol. 24, no. 2 SE-Article, pp. 115–127, Mar. 2024, doi: 10.31172/jmg.v24i2.1049.
8. G. Urgilés, R. Célleri, J. Bendix, and J. Orellana-Alvear, "Identification of Spatio-temporal Patterns in

Extreme Rainfall Events in the Tropical Andes: A Clustering Analysis Approach," *Meteorol. Appl.*, 2024, doi: 10.1002/met.70005.
9. C. C. Ibebuchi, "Large-scale Forcing Over the Homogeneous Regions of Summer Rainfall Anomalies in Southern Africa," *Meteorol. Appl.*, 2023, doi: 10.1002/met.2114.
10. F. Mekanik, M. A. Imteaz, S. Gato-Trinidad, and A. Elmahdi, "Multiple Regression and Artificial Neural Network for Long-Term Rainfall Forecasting Using Large Scale Climate Modes," *J. Hydrol.*, 2013, doi: 10.1016/j.jhydrol.2013.08.035.
11. E. Aldrian and Y. S. Djamil, "Spatio-temporal climatic change of rainfall in East Java Indonesia," *Int. J. Climatol.*, vol. 28, no. 4, 2008, doi: 10.1002/joc.1543.
12. P. Narayanan, A. Basistha, and S. Kamna, "Understanding Trends and Shifts in Rainfall in Parts of Northwestern India Based on Global Climatic Indices," *Weather*, 2016, doi: 10.1002/wea.2746.
13. B. J. Abiodun, S. A. Omar, C. Lennard, and C. Jack, "Using Regional Climate Models to Simulate Extreme Rainfall Events in the Western Cape, South Africa," *Int. J. Climatol.*, 2015, doi: 10.1002/joc.4376.
14. M. K. Roxy *et al.*, "A Threefold Rise in Widespread Extreme Rain Events Over Central India," *Nat. Commun.*, 2017, doi: 10.1038/s41467-017-00744-9.
15. V. Hari, S. Karmakar, and S. Ghosh, "Diametric Changes in Trends and Patterns of Extreme Rainfall Over India From Pre-1950 to Post-1950," *Geophys. Res. Lett.*, 2013, doi: 10.1002/grl.50631.